JOURNAL OF OPTOELECTRONICS AND ADVANCED MATERIALS Vol. 16, No. 3 - 4, March – April 2014, p. 494 - 498

n-β-$FeSi_2$/p-Si heterojunction solar cells simulation by AFORS-HET

W. Y. XU, F. X. CHEN*, J. F. WANG
Department of physics science and technology, Wuhan University of Technology, Wuhan, 430070, China

The semiconducting iron disilicide β-$FeSi_2$ has recently attracted considerable attention due to its remarkable optical and electrical properties. In this paper, we investigate the β-$FeSi_2$/c-Si(p)/μc-Si(p^+) heterojunction solar cells and optimize its structure by AFORS-HET software. By adjusting the emitter and back surface field (BSF) parameters, we find that increment of the emitter thickness would decrease the short current density and the conversion efficiency; the influence of the interface state could not be ignored; an optimized BSF will increase 1 point of conversion efficiency. The final optimized parameters of heterojunction solar cell are V_{oc}=600.8 mV, J_{sc}=40.81 mA/cm^2, FF=80.77% and η=19.8%.

(Received January 15, 2013; accepted March 13, 2014)

Keywords: $FeSi_2$, Heterojunction solar cell, AFORS-HET

1. Introduction

β-$FeSi_2$ is an attractive semiconductor owing to its extremely high optical absorption coefficient ($\alpha > 10^5$ cm^{-1}), and is expected to be an ideal material for a thin film solar cell [1]. Generally the optical absorption coefficient of β-$FeSi_2$ is 10^5 cm^{-1} corresponding to photon energy beyond 1 eV and reaches to the peak coefficient 2.67×10^5 cm^{-1} when photon energy is 6.26 eV. And a 1μm-thick β-$FeSi_2$ film absorbs almost all of the sunlight [2]. The β-$FeSi_2$ films can be epitaxially grown on the silicon surface and well matched with silicon devices in fabricating techniques. Besides this, β-$FeSi_2$ solar cell also can be integrated as a module similar to thin film silicon solar cell. So it is preferable to employ low cost β-$FeSi_2$ film solar cell in PV industry.

In experiment, β-$FeSi_2$ thin film was demonstrated to be used in heterojunction structure [3]. But the conversion efficiency of cells mentioned in literatures is not good, there is a great potential space to be improved [4-7]. In this article, the AFORS-HET software [8] was used to simulate the I-V characteristics of n-β-$FeSi_2$/p-Si/μc-Si(p^+) heterojunction solar cells. The simulation results showed that the optimal thickness and doping concentration of β-$FeSi_2$ film were 2 nm and 8×10^{20} cm^{-3}, respectively. Moreover, the computation results indicated that interface defect states had critical influences on cell performances. In addition, BSF could increase conversion efficiency effectively compared with solar cell without BSF. All these indicate that n-β-$FeSi_2$/p-Si/μc-Si(p^+) heterojunction is a good potential structure for photovoltaic applications.

2. Structure of the heterojunction solar cells

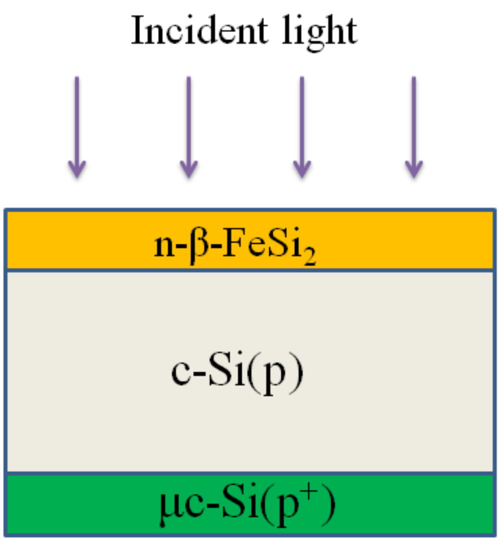

Fig. 1. Schematic diagram of n-β-$FeSi_2$/p-Si/μc-Si(p^+) heterojunction solar cell.

The structure of n-β-$FeSi_2$/p-Si/μc-Si(p^+) solar cell is shown in Fig. 1. The top layer is a β-$FeSi_2$ film, with variable thickness from 1 nm to 10 nm and adjustable doping concentration. The bottom one is a μc-Si layer, which forbidden band gap is fixed at 1.4 eV [9] and thickness varies from 2 nm to 20 nm. The p-type layer is mono-crystalline silicon.

Table 1. Parameters used in simulation.

	n-β-$FeSi_2$	c-Si(p)	μc-Si(p^+)
Thickness (nm)	Adjustable	3×10^5	Adjustable
Dielectric constant	31	11.9	11.9
Electron affinity (eV)	4.71	4.05	4
Band gap (eV)	0.87	1.12	1.4
Effective conduction band density (cm^{-3})	1.7×10^{18}	2.8×10^{19}	10^{20}
Effective valence band density (cm^{-3})	1.7×10^{18}	1.04×10^{19}	10^{20}
Electron mobility ($cm^2V^{-1}s^{-1}$)	206	1041	10
Hole mobility ($cm^2V^{-1}s^{-1}$)	168	412	3
N_D (cm^{-3})	Adjustable	0	0
N_A (cm-^{3})	0	10^{16}	Adjustable

In simulation, the default values are used for the defects in c-Si(p) layer. The parameters of β-$FeSi_2$ layer are cited from Ref. [10]. All initial parameters are listed in Table 1. The simulated illumination condition is AM1.5 with temperature 300 K.

3. Results and discussion

3.1 Influences of the emitter thickness

The role of emitter layer is to create a built-in electric field with the base region, and allow incident light enter into the base region as more as possible. If the thickness of β-$FeSi_2$ layer increases, which means the incident absorption in n-layer increases, the photocurrent should increase too. But there is a premise that the minority carrier lifetime in β-$FeSi_2$ film should be long enough. Otherwise, the electron-hole pairs can't be collected by PN junction. Therefore, the thickness of β-$FeSi_2$ film must be limited by minority carrier diffusion length. On the other hand, the series resistance seriously affects the output characteristic of solar cell. The series resistance increases with the increase of the emitter thickness, which leads to decline of the fill factor (FF) and conversion efficiency (η)[11].

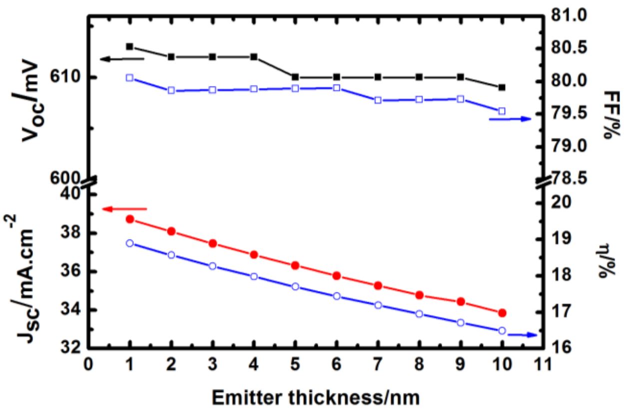

Fig. 2 The effect of emitter thickness on performances of the heterojunction solar cells.

Fig. 2 lists the variation of parameters with the emitter thickness. In Fig. 2, we find that the open circuit voltage (V_{oc}) decreases slowly, while the short circuit current (J_{sc}) drastically decreases with the increase of emitter thickness. The reason is that with the emitter thickness increases, the number of photons absorbed in emitter layer increases too. While there are a large number of recombination centers and it lacks electric field in emitter region, photogenerated carriers in this region can't reach the edge of potential barrier and contribute to photocurrent. The excess carriers will disappear because of recombination, which results in the decrease of J_{sc}. The FF gradually decreases with increasing n-layer thickness, mainly because of the increases of series resistance [12]. For V_{oc}, generally

$$V_{oc}=\frac{k_0T}{q}[\ln(J_{sc}/J_0)+1],$$

where T is temperature, k_0 Boltzmann constant, q electron charge, J_0 reverse saturated current. When J_{sc} decreases, the V_{oc} drops slowly. Finally, solar cell with efficiency 18.57% is obtained with optimum emitter thickness 2 nm.

3.2 Effect of emitter layer doping concentration

The emitter doping concentration is another key parameter of heterojunction solar cells. If the doping concentration is known, the performances of a solar cell can be easily judged. In order to collect photogenerated carriers as more as possible, the diffusion length of the minority carriers should be extended. While increasing doping concentration equals to increase recombination and decrease the minority carrier diffusion length, which reduces photogenerated carrier collection efficiency and declines J_{sc}. From this point, a lower doping concentration is better. However, in view of V_{oc}, the doping concentration should be as high as possible. So it seems hard to improve both J_{sc} and V_{oc} at the same time by adjusting the doping concentration.

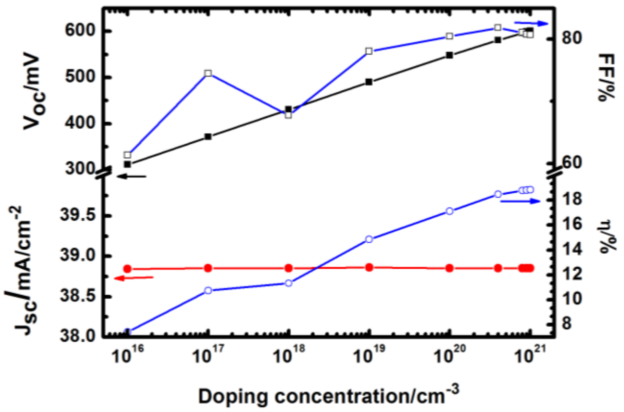

Fig. 3. The effect of different emitter layer doping concentration on performances of the heterojunction solar cells.

The variations of parameters on the doping concentration are shown in Fig. 3. It can be seen from Fig. 3, with increasing the emitter doping concentration, V_{oc} and FF significantly increase except J_{sc}. And the conversion efficiency increases firstly, then it saturates at 8×10^{20} cm^{-3}, due to the heavy doped defects and Auger recombination effect. Furthermore, heavy doping concentration will result in a "dead layer", photogenerated carriers in this layer almost combine, leading to the drop of efficiency. Hence, the emitter layer doping concentration should be controlled at 8×10^{20} cm^{-3}.

3.3 Impact of the interface states in solar cell

The discussions above are ideal situations. Actually we can't ignore the effect of interface states density on the cell performances in practical production process. Here an ultrathin c-Si layer model is used as interface defect, with continuous donor and acceptor states in the band-gap.

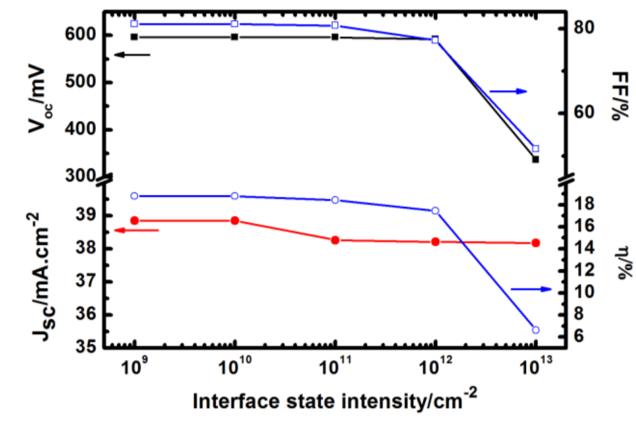

Fig. 4. The effect of interface state density on performances of heterojunction solar cells.

Fig. 4 shows the effect of interface state density on performances of heterojunction solar cells. As described in Fig. 4, when the interface states density (D_{it}) is less than 10^{10} cm^{-2}, the solar cell performances are almost unaffected, and conversion efficiency is maintained at about 18.78%, which is close to the efficiency with no interface state; when the interface states density is over 10^{10} cm^{-2}, both V_{oc} and J_{sc} decline. When D_{it} increases from 10^{10} cm^{-2} to 10^{13} cm^{-2}, the V_{oc} declines from 596.1 mV to 336.7 mV, and J_{sc} declines from 38.85 mA/cm^2 to 38.18 mA/cm^2. When D_{it} is 10^{13} cm^{-2}, conversion efficiency rapidly reduces to 6.63%. The reduction of V_{oc} is mainly due to increment of PN junction inverse saturation current. With interface defect density increases, the recombination of excess carrier also increases, which results in the increase of reverse saturation current and reduces V_{oc} and FF. So passivation technology is important for high efficiency solar cells, such as plasma assisted H passivation, which is used to control the interface defect density lower than 10^{10} cm^{-2}.

3.4 Effect of BSF structure

BSF refers to a region of producing barrier effect to photogenerated carriers, and reduces the carrier recombination rate at this region. The barrier can not only improve the photocurrent, but also improve photovoltage to some extent [13]. Similar with crystalline silicon cells, BSF can be achieved by a layer with same doping type as the absorbing layer, but with higher doping concentration. Because microcrystaline silicon is the mixed phase of nanocrystalline silicon and amorphous silicon, it simultaneously owns high optical absorption coefficient and good stability. Furthermore its band gap is adjustable with the crystalline phase, and easy to realize optimal parameters as designed. So in this paper, the microcrystalline silicon is chosen in BSF structure [14].

The influences of the BSF thickness on performances of heterojunction solar cells are shown in Table 2. We note that all the parameters are unchanged with thickness increases. This is very beneficial. In production, it is very difficult to grow thicker microcrystalline silicon films because of low growth rate. If the requirement of BSF layer is not thick, this will save a lot of time. Therefore it is possible to set the BSF thickness at 5 nm.

Table. 2. The photovoltaic performances of heterojunction solar cells with different BSF thickness.

Thickness/nm	V_{oc}/mV	J_{sc}/mA·cm^{-2}	FF/%	η/%
2	600.80	40.76	80.76	19.78
5	600.80	40.76	80.76	19.78
10	600.80	40.76	80.76	19.78
15	600.80	40.76	80.76	19.78
20	600.80	40.76	80.76	19.78

Fig. 5 listed the effect of different BSF doping concentration on performances of heterojunction solar cells. It is found that BSF plays a positive role in improving cell performances. The effect of BSF is not obvious with lower doping concentration. While when the doping concentration is over 10^{19} cm^{-3}, the conversion efficiency reaches 19.8%. After that with the doping concentration further increases, the efficiency has no improvement. Though barrier effect for carrier transport can be reduced by increasing the doping concentration, this also shows that a high doping concentration is a good guarantee for BSF. Because of its specific crystal phase, microcrystalline silicon has the possibility of higher doping concentration, which is one of the reasons why microcrystalline silicon is chosen as BSF here.

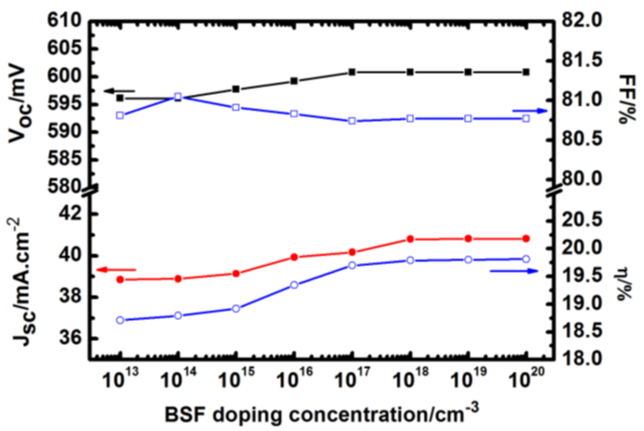

Fig. 5. The effect of different BSF doped concentration on performances of heterojunction solar cells.

Fig. 6 lists a comparison of J-V curves for heterojunction solar cells with and without BSF. As shown in Fig. 6, after adding BSF, all parameters of heterojunction solar cells are improved, which shows a reasonable BSF, especially optimal BSF doping concentration can improve the conversion efficiency of solar cells effectively. The detailed data were listed in Table 3.

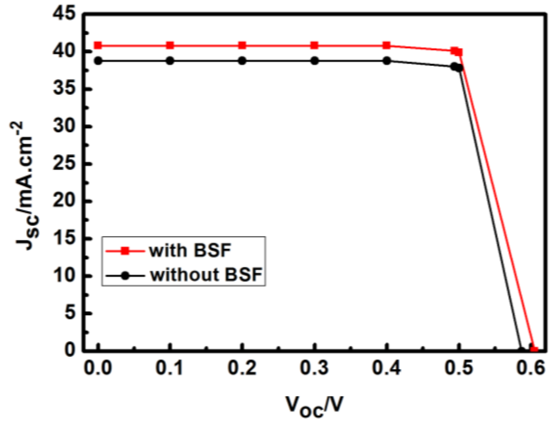

Fig. 6. The J-V characteristics of heterojunction solar cells with and without BSF.

Table 3. The comparisons of heterojunction solar cells with and without BSF.

Type	V_{oc}/mV	J_{sc}/mA·cm^{-2}	FF/%	η/%
n/p	596.10	38.85	81.07	18.78
n/p/p$^+$	600.80	40.81	80.77	19.80

In Table 3, we find that a reasonable BSF increases the conversion efficiency about 1 percent. This verifies the p/p$^+$ junction has two major roles: on the one hand, it inhibits the back surface recombination, which decreases the reverse saturated current and increases V_{oc}; on the other hand, it encourages the electron-hole pair collection in PN junction, which improves the spectral response in long wavelength band and increases J_{sc}.

4. Conclusions

In this paper, the AFORS-HET software is used to simulate n-β-$FeSi_2$/c-Si(p)/μc-Si(p$^+$) heterojunction solar cells. The influences of emitter, interface state and BSF are discussed. The computation results show that the thicker n-layer will lower the J_{sc}. Interface state has a greater impact on cell performances, so it is necessary to control the interface defect density lower than 10^{10} cm^{-2} to improve the conversion efficiency. BSF thickness has little effect on cell efficiency. While reasonable BSF doping concentration effectively improves the conversion efficiency. The optimized results of heterojunction solar cells are: the thickness of n-layer is 2 nm, with doping concentration 8×10^{20} cm^{-3}; the thickness, doping concentration for BSF are 5nm and 10^{19}cm^{-3}, respectively. And the final J-V parameters of the heterojunction solar cell are V_{oc}=600.8 mV, J_{sc}=40.81 mA/cm^2, FF=80.77%, η=19.8% .

Acknowledgements

This paper is supported by the "Fundamental Research Funds for the Central Universities" (Grant Nos. WUT 2013-Ia-004 and WUT 2012-Ia-031) .

References

[1] Y. Fukuzawa, T. Ootsuka, N. Otogawa, et al. Photonics for Solar Energy Systems, **6197**(2006).
[2] M. C. Bost and J. E. Mahan. Journal of Applied Physics, **58**, 2696 (1985).
[3] S. L. Liew, Y. Chai, H. R. Tan et al., Journal of The Electrochemical Society, **159**(1), H52, (2012).
[4] Z. X. Liu, M. Watanabe, M. Hanabusa. Electrical and photovoltaic properties of iron-silicide/silicon heterostructures formed by pulsed laser deposition. Thin Solid Films, **381**, 262 (2001).
[5] Z. X. Liu, S. N. Wang, N. Otogawa, et al., Solar Energy Materials & Solar Cells, **90**, 276 (2006).
[6] M. Shaban, K. Nakashima, W. Yokoyama, et al., Journal of Applied Physics, **46**, L6667 (2007).
[7] G. K. Dalapati, S. L. Liew, A. S. W. Wong, et al., Applied Physics Letters, **98**, 013507 (2011).
[8] L. S. Wang, F. X. Chen, J. Optoelectron. Adv. Mater. **3**(1), 87 (2011).
[9] A. A. Boussettine, B. Rezgui, A. Benmansour et al., Revue des Energies Renouvelables, **13**(1), 179 (2010).
[10] L. W. Wang, L. H. Qin, Y. X. Zheng, et al., Applied Physics Letters, **65**, 3105 (1994).
[11] C. Yu, G. F. Hou, F. Liu, et al., Journal of synthetic crystals, **38**, 662 (2009).
[12] B. Y. Ren, M. H. Wang, X. P. Liu, et al., Acta energlae solaris sinica, **29**, 125(2008).
[13] L. Zhao, C. L. Zhou, H. L. Li, et al. Acta Physica Sinica, **57**, 3212 (2008).
[14] L. M. Li, B. Q. Zhou, X. Chen, et al., Information recording materials, 10, 18(2009).

*Corresponding author: phonixchen79@aliyun.com